DOI: 10.13009/EUCASS2022-6184

Hydrogen Peroxide Decomposition: Testing and Characterization of MnOx-based Catalysts

Stefania Carlotti and Filippo Maggi
Politecnico di Milano
Dept. Aerospace Science and Technology, Via La Masa 34, Milano, Italy

stefania.carlotti@polimi.it · filippo.maggi@polimi.it

Abstract

The aim of this work is to present the overall catalysts production, characterization and testing processes initiated at the Space Propulsion Laboratory of Politecnico di Milano in the framework of high-test peroxide catalytic decomposition studies. Three procedures based on an impregnation process using potassium permanganate as precursor in aqueous solution and commercial aluminum oxide as support, have been investigated to evaluate the possibility of lifetime increasing of a catalytic bed. In this respect, single pellets have been tested at lab-scale level to evaluate the effect of subsequent decomposition runs and identify their end-of-life. Additionally, a preliminary experimental campaign involving produced MnOx/Al_2O_3 pellets enabled to verify the decomposition efficiency and the catalysts consumption in relevant conditions. A temperature-efficiency of 88% was achieved during the steady state regime and, after 36 seconds of cumulative firing, the catalysts showed limited degradation in terms of performance and wearing.

1. Introduction

Nowadays, the research towards green alternatives to the most widely employed propellants, such as hydrazine and nitrogen tetroxide/monomethylhydrazine (NTO/MMH), is greatly increased, pushed by a worldwide shared interest for improved environmental safety and consequent economic benefits [1]. Hydrogen peroxide is considered one of the best candidates for near-future storable and green space propulsion, because of the advantages of low toxicity, low environmental impact, and because its decomposition produces no pollutant species. Pure hydrogen peroxide can exothermically decompose into water vapor and oxygen according to the reaction listed in Eq. (1):

$$2H_2O_{2(l)} \rightarrow 2H_2O_{(g)} + O_{2(g)} + heat \qquad \textbf{(1)}$$

The adiabatic decomposition predicted by thermochemistry can produce hot gases at a temperature range of 898-1269 K, depending on the H_2O_2 concentration (85-100%). Then, the hot decomposition products can be directly expanded in a nozzle or injected in a combustion chamber to react with a solid or liquid fuel. In the former case, exploiting a monopropellant configuration, high-test hydrogen peroxide can deliver specific impulse between 150 and 180 seconds, while in a bipropellant rocket system, more than 300 seconds can be achieved [2].

The most reliable methods to facilitate the decomposition is lowering the energy threshold by employing suitable catalysts [3][4]. Hence, one of the most important technology challenges in the realization of hydrogen peroxide-based rockets is the development of reliable and efficient catalysts [4]-[6]. The catalyst has to fulfil several requirements, such as high stability, longevity and short response time. Moreover, it has to provide reproducible performance in a wide range of operating conditions, spanning from high-test peroxide (HTP) liquid injection at high pressure to the resulting decomposition products at elevated temperature. Additionally, long-term stability, high thermal and mechanical strength associated with ignition/shut down cycles, as well as low cost are typical features required from catalysts.

Hence, it is clear that the choice of the most suitable catalyst is not straightforward, since trade-offs must be taken into account. Activity and strength are inversely correlated, with high-surface area supports being more susceptible to cracking [11]. In fact, the common gauzes or wire meshes, despite the high mechanical strength, are characterized by short residence time and poor performance, while pelletized beds typically enable operations with large mass flow rate and low pressure drop at the cost of a lower mechanical strength [4].

Nowadays, different metals and/or metallic oxides (such as silver [7], platinum [8][9], iron oxides [10], manganese oxides (MnOx) [3][11]-[14] and others [4]) have been investigated as the active phase. Among the others, manganese oxides-based catalysts represent an interesting yet cheap solution, demanding thorough analysis regarding their

DOI: 10.13009/EUCASS2022-6184

characteristics and their production technique. Additionally, the catalyst bed investigations need to be coupled with the optimization of the mass and configuration of new thrusters, thus, opening the door to the detailed analysis of high-test peroxide-based (HTP) prototypes [11][15-20].

The aim of this work is to present the studies currently performed at the Space Propulsion Laboratory of Politecnico di Milano about the catalysts based on manganese oxides for the decomposition of hydrogen peroxide. In particular, a procedure for catalyst preparation based on an impregnation process using potassium permanganate as precursor in aqueous solution and commercial aluminum oxide as support, is proposed. Pellets reactivity and lifetime are quantified by investigating the decomposition of a defined amount of HTP at lab-scale level and a preliminary experimental campaign in relevant conditions in a decomposition chamber is presented.

2. Propellant, Catalyst and Catalytic Support

The HTP used for testing is the PROPULSE®875 by Evonik. At the time of testing the actual concentration was ~83.5%, determined by a titration against potassium permanganate at acidic conditions. Grade reduction is attributed to natural aging since its original supply in 2019. The liquid was stored under laboratory-controlled conditions (about 25 °C) inside its original aluminum containers. The precursor used for catalyst preparation is potassium permanganate, 99% purity in crystalline form from Alfa Aesar (CAS number 7722-64-7), while trimodal α-alumina spheres by Alfa Aesar (CAS number 1344-28-1) have been used as ceramic support. They are relatively large pellets, with a mean diameter of 4.76 mm and low surface area (~ 0.82 m^2/g).

The catalysts were manufactured according to three impregnation methodologies, named as in the following:

- *Baseline procedure*: (i) pre-treatment of the virgin carrier by calcination at 500°C for 1 h (~150 pellets) ; (ii) wet impregnation with distilled water solution of 6wt% potassium permanganate for 3 h at 50°C under controlled agitation (see Figure 1(a)); (iii) ultrasound washing of the spheres for 15 minutes every hour; (iv) drying in an oven set at 120°C for 30 minutes; and (v) calcination at 550°C for 1 h (heating rate: ~15 °C/min, cooling rate ~20 °C/min).
- *1-step procedure*: it is almost the same as the baseline procedure apart from the wet impregnation step which lasts only 1 hour.
- *3-step procedure*: it consists of three subsequent impregnation and calcination process, repeating the 1-step procedure three times.

The active phase content was determined by the so-called catalyst loading, evaluated as the percent mass increase of the support after preparation. Results are shown in Table 1. The baseline and the 1-step procedure are almost equivalent, possibly suggesting that long impregnation times are not necessary to get a mass loading increment with this kind of low surface area support. On the contrary, the 3-step procedure suggests that a stratification of the active phase is occurring, increasing the amount of active phase. However, the strength of the formed chemical bond must be verified to avoid unwanted detachment of MnOx during the early phase of the decomposition process, resulting in fines, that increase the reaction rate, and unwanted consumption of the catalysts.

Table 1: Mass loading for the tested impregnation procedures.

Procedure	**Mass loading, %**
Baseline	1.90
1-step procedure	1.92
3-step procedure	4.8


(a) (b) (c)

Figure 1: Catalysts produced according to (a) baseline procedure; (b) 1-step procedure; (c) 3-step procedure.

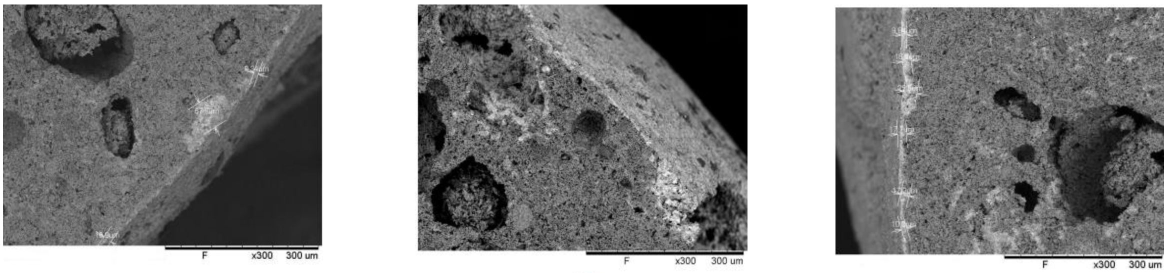

(a) (a) (a)

Figure 2: SEM images of the active phase layer for catalysts produced according to (a) baseline procedure; (b) 1-step procedure; (c) 3-step procedure.

As shown in Figure 1, the procedure involving subsequent impregnation, drying and calcination steps result in a more homogeneous distribution of the active phase on the supports surface, as qualitatively indicated by the uniform surface colour. The effectiveness of the 3-step methodology is confirmed also by SEM images obtained by means of a Hitachi RTM3000 Scanning Electron Microscope, showing the cross section of the produced catalysts (refer to Figure 2). As far as the first two methodologies are concerned, the low porosity of the support leads to very thin (i.e, few microns thick) and not uniform active phase layer, which results larger and uniformly distributed in the 3-step case.

3. Test Apparatus

3.1 Endurance Tests

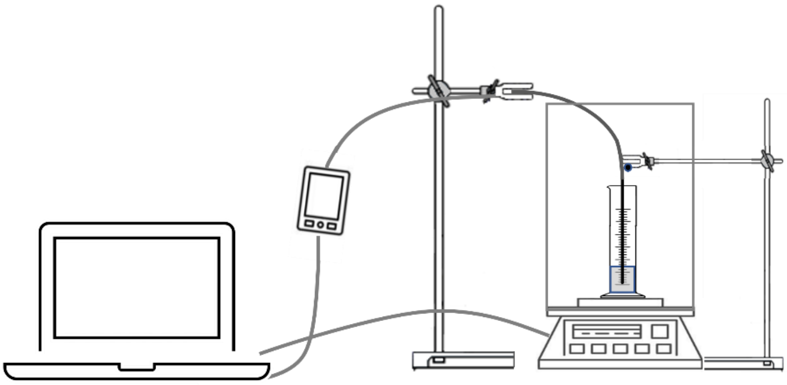

Figure 3: Endurance tests apparatus.

DOI: 10.13009/EUCASS2022-6184

Lifetime of the catalysts has been characterized by a dedicated test apparatus, shown in Figure 3, inspired by the work of Palmer [20]. A 25 mL graduated cylinder is placed on a Gibertini®Crystal digital lab scale under a fume hood. The scale connects to a logger over its serial port, transmitting the instantaneous mass measurement at a frequency of about 5 Hz. The cylinder contains ~3 g of HTP, the temperature of which is monitored by a T-type thermocouple (see Table 1 for details) connected to a TC-08 thermocouple USB data logger (by Pico Technology, up to 100 ms per channel). A single catalyst is dropped in the cylinder per run, and the increase of HTP temperature and its mass loss, as steam, oxygen and peroxide vapour form, are monitored. Before and after the test, each sample is dried for 30 minutes in the oven to remove any trace of moisture. The experiment can be considered concluded whether the final HTP mass is stable across 1 minute interval or if the onset of the reaction exceeds 300 s. In the latter case the catalyst can be considered to have reached the End-Of-Life (EOL).
Ideally, the mass variation rate equals the consumption rate of reactants, and therefore the reaction rate. However, some gaseous products condense on the sides of the cylinder; thus, lowering the reaction rate and diluting the original hydrogen peroxide. Nevertheless, the present approach is simple and allows to collect qualitative and quantitative data for comparison purposes.

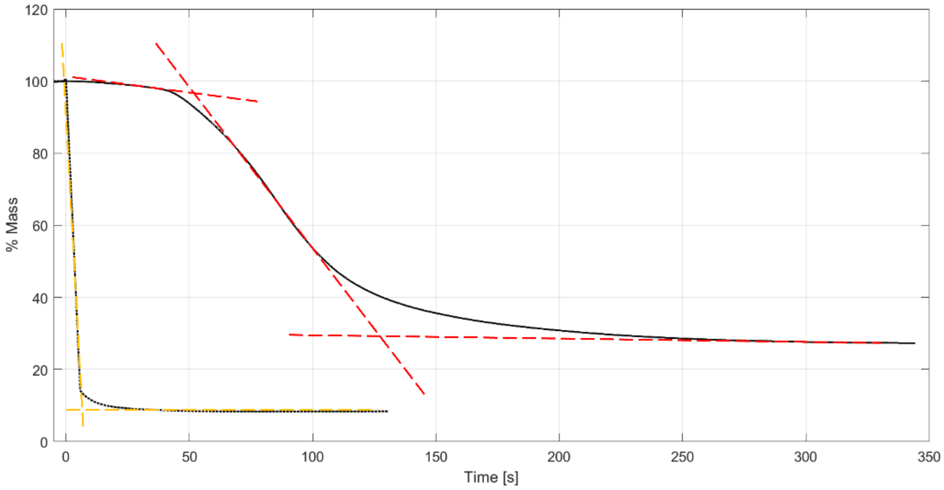

Figure 4: Examples of algorithm application on regular and fast decompositions (black curves). The dashed lines mark onset and endset computation.

A “regular” mass loss history (see solid black line in Figure 4) is characterized initially by a slow mass decrease, that can be approximated with a linear trend. This induction of the reaction may last several minutes, depending on the catalyst’s activity, or being even absent. Catalysts releasing dusts during the reaction are characterized by extremely high activity, leading to fast decomposition without induction time (see dotted black line in Figure 4). Similarly, highly active catalysts generally have a small initiation, typically caused by the bouncing of the pellets, propelled by the decomposition gases, on HTP free surface. In this case, the initiation is caused by the reduced contact with the liquid free surface, slightly delaying the reaction onset. This phenomenon is absent for pellets with low activity, that appear to be fully submerged throughout the entire decomposition. The second step of the decomposition process is characterized by a fast decrease of HTP mass, leading to the maximum reaction rate, observable as a steep linear region. As the decomposition proceeds, the reaction rate decreases until the HTP mass consumption ends.

A post-processing algorithm is implemented to evaluate the reaction rate. The algorithm computes the representative reaction rate for each pellet by approximating the straight sections of the reaction with linear fits, the intersection of which identifies the onset and endset of the reaction (see Figure 4). Then, it can be computed according to Eq. (2).

$$r = \frac{m(t_{end}) - m(t_{start})}{t_{end} - t_{start}} \tag{2}$$

In the case of “regular” reaction, three lines are needed for the reaction rate computation (see red dotted lines in Figure 2): (i) the first line takes into account the first 5% of the mass history, starting from t = 0; (ii) the second line considers a ±5% interval around the point of maximum reaction rate; (iii) the last 5% of the mass history is fitted by the third line. The intersection between the former two lines identifies the reaction onset t_{start} , while the latter two lines enable to quantify the end of reaction. In the case of “fast” decomposition, the onset of the reaction is t = 0, while the ending time is computed as already described (see the yellow dotted lines in Figure 4).

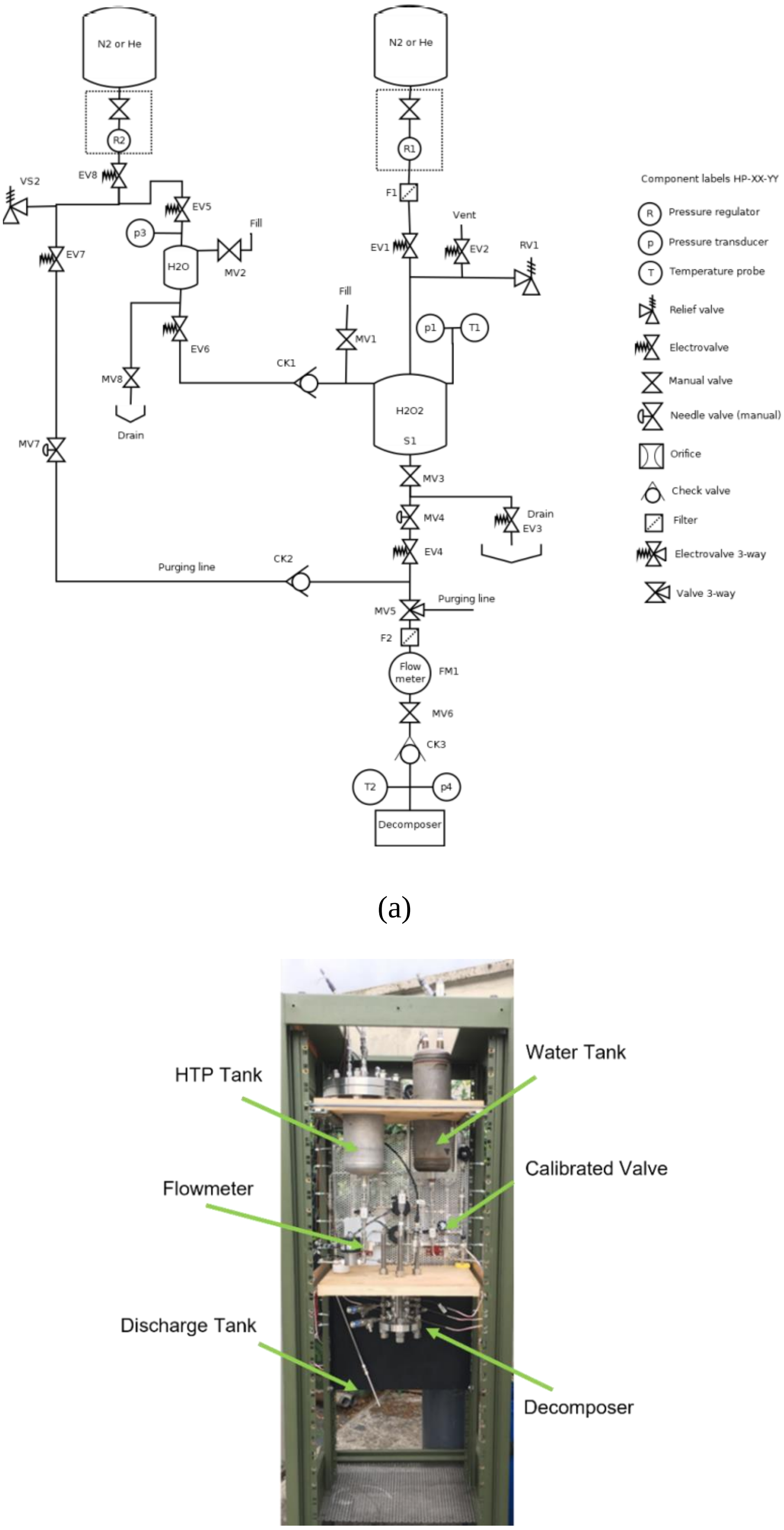

(a)

(b)

Figure 5: HyPer facility: (a) experimental scheme and (b) picture of the test bench assembly.

3.2 Decomposer Assembly

The experimental characterization of the catalytic decomposition chamber (DCm) has been carried out using SPLab Hydrogen Peroxide Test Facility (HyPer). The test bench is intended for easy adaptation to test different engine configurations (i.e., monopropellant, bipropellant, hybrid rockets) and operating conditions (i.e., operating pressures, mass flow rate, etc). The scheme of the experimental apparatus and a picture of the HyPer test rig are provided in Figure 5.

High-test peroxide is stored at up to 35 bar pressure in the main tank made of passivated stainless steel and employing PTFE seal. The tank is connected to a relief valve to avoid uncontrolled overpressure, while a second safety protocol can be manually activated in case of dangerous temperature rise. In fact, the control block can enable the flooding of the HP tank by water, which is stored in a separate tank at up to 40 bar pressure, thus diluting its concentration, while simultaneously draining the tank.

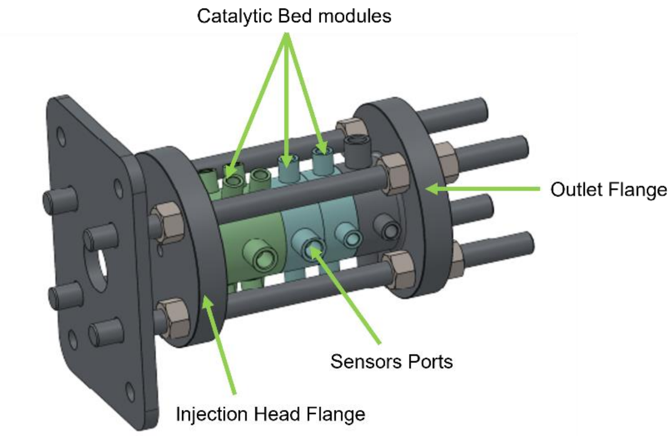

(a)

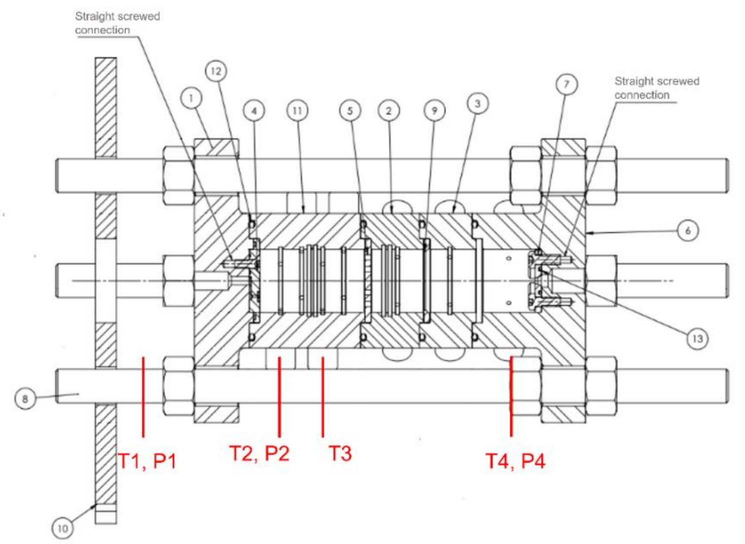

(b)

Figure 6: Decomposition chamber assembly: (a) main components; (b) cross-section with measurement location nomenclature.

Temperature and pressure of the propellant are continuously monitored by means of a T-Type thermocouple and a pressure transmitter (refer to Table 2 for details). A calibrated needle valve and a turbine flowmeter are placed along the hydrogen peroxide feeding line to regulate the flow and measure the propellant mass flow rate, while a check valve prevents reverse flow. Gaseous nitrogen is used for propellant tank pressurization, purging and venting all fluidic lines. The DCm prototype, shown in Figure 6, has been designed in a modular manner to grant easy replacement and high operating flexibility. It consists of five main components realized in Inconel: three catalytic bed modules (2,3,11) and the injection (1) and outlet flanges (6). Housed in the injection head component, a shower head plate (4) with three recessed holes of 1 mm diameter enables the injection of liquid hydrogen peroxide into the catalytic packed bed, while an exit orifice in the outlet flange regulates the chamber pressure. The catalytic bed is packed between the injection plate and a retainer grid (also called distribution plate (5)). A total of 22 ports are planned for housing N-type thermocouples and up to five pressure transmitters. The temperature sensors can be distributed both axially and radially, enabling the tracking of the temperature profiles at different locations and the evaluation of possible channeling phenomena leading to non-uniform decomposition. Main characteristics of the DCm prototype are listed in Table 3.

Table 2: SPLab HyPer test rig sensors list.

	Location	**Model**	**Main Characteristics**
Thermocouples T-type	HTP and water tank, HTP Pre-injection	Diam. 3 mm, minerally-insulated by TC Direct	Maximum Working Temperature: 370 °C Characteristic Times: 0.7 s
Thermocouples N-type	Decomposer	Diam. 1 mm, minerally insulated by TC Direct	Maximum Working Temperature: 920 °C Characteristic Times: 0.2 s
Pressure Transducers	HTP tank HTP Pre-injection Decomposer	Pressure Transmitters by Trafag	Pressure Range: 0-40 bar (overpressure 120 bar, burst 300 bar) Measurement accuracy 0.3% F.S. at 25°C
Turbine Flowmeter	Supply line	915 Titan turbine flowmeter	Flow range: 0.12 -1.5 l/min Linearity: 2% FSD Operating Temperature range: -25 - 125°C Operating Pressure range: 0 - 40 bar

Table 3: Main Characteristic of the DCm prototype.

Inner Diameter	30 mm
L/D ratio	~ 2 ÷ 4
Exit Orifice Diameter	2.5 - 3 mm
Injection Holes Diameter	1 mm

4. Results and Discussion

4.1 Endurance Tests

Endurance tests provide significant insight into the lifetime of the produced catalysts. The continuous flooding of liquid hydrogen and the progressive consumption of the catalysts can be considered representative of the upper part of a real decomposer assembly, thus providing indication on the progressive deterioration of performance in terms of rising times and temperature efficiency for a fixed length of the catalyst bed.

An example of the outcome of the performed endurance tests is reported in Figure 7. A pellet of initial mass $m_p = 0.078$ g, produced according to the 1-step impregnation procedure, was able to perform six successful decomposition runs before reaching EOL (i.e., onset time > 300 s). The first tests exhibit the already mentioned “fast” decomposition behaviour, progressively decreasing the maximum reaction rate, and increasing the onset time with the number of the run. Similarly, as the catalyst activity decreases, a larger amount of hydrogen peroxide does not readily react. In fact, when catalyst loses reactivity almost half of the original hydrogen peroxide mass remains in the cylinder.

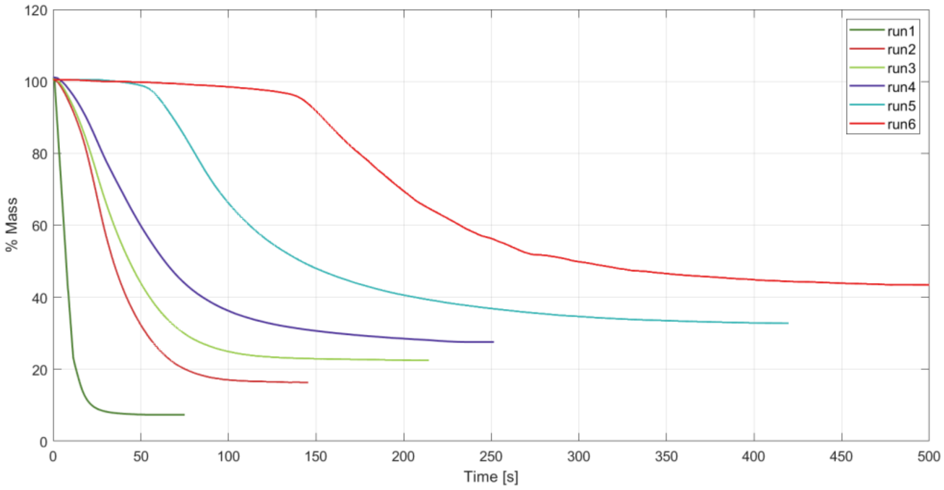

Figure 7: Example of endurance test: 1-step production catalyst.

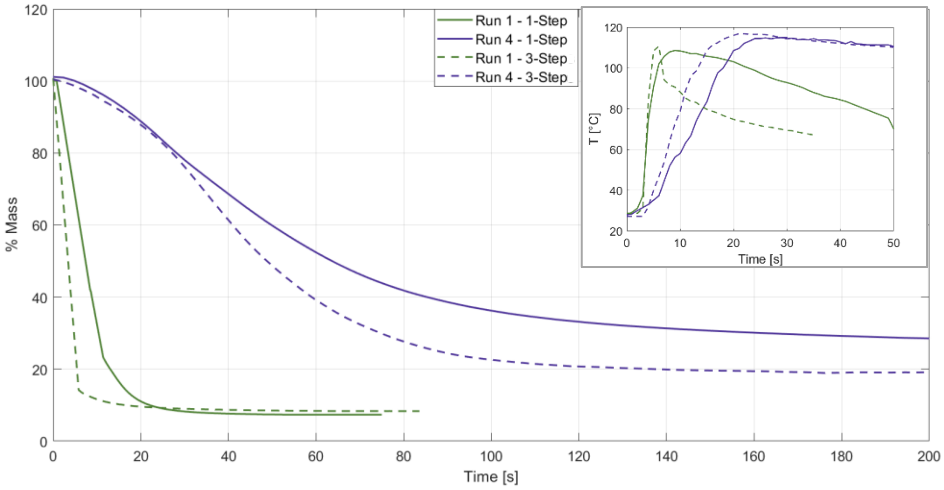

Figure 8: 1-Step and 3-Step catalyst mass history comparison.

A comparison between the same runs (i.e., run 1 and run 5) of two pellets produced considering the 1-step and 3-step impregnation methods has been conducted. It is worth underlining that the following results shall be considered as qualitative indication since they are based on the decomposition runs of a single catalyst per production batch. Thus, absolute quantification and final considerations demand further investigation and a statistical analysis. Nevertheless,

useful indications can be derived from these initial tests. To increase data reliability, catalysts of equal initial mass (i.e., $m_p = 0.078$ g) have been selected in order to avoid spurious effects on the onset time due to a different "nominal" exposed surface. Mass and temperature histories are shown in Figure 8. Structural integrity of pellets between runs was verified by means of microscope and SEM visualization.
Fast decomposition is confirmed for both the catalysts, with the 3-step one characterized by higher reaction rate. Both the 3-steps and the 1-step catalysts successfully decompose almost 90% of HTP during run 1. On the contrary, during run 5, the latter shows a lower decomposition efficiency, indicating the progressive consumption of the catalytic material. In fact, run 6 represents the EOL for the 1-step catalyst, while the reaction rate for the 3-step one (see Figure 9) indicates that the catalyst may be used for other decomposition runs, even though a limited efficiency is obtained.
Typical evolutions of liquid HTP are shown in Figure 8. It must be noted that fast decomposition, which governs the first runs, led to a steep temperature increase, possibly vigorously displacing the thermocouple against the graduated cylinder walls, and, hence, affecting the measurement. However, trends similar to those derived by mass histories can be observed. Finally, the temperature never exceeds 120°C, providing an indication of partial boiling of the solution. The difference with respect the nominal boiling temperature of 83.5% concentration (~ 130°C) can be attributed to thermal loss and to the dilution process due to steam condensation.

It is worth underlining that comparing the reaction rate cancels out the uncertainties related to different onset times - see Eq. (2) – that may lead to unsuccessful analyses if referred only to the mass history, since several aspects (such as the catalyst mass and volume, amount of HTP, condensation phenomena, etc.) may affect this parameter. Hence, the reaction rate analysis can be approached as a more reliable, although not exhaustive, methodology for the assessment of catalysts endurance. According to Figure 9, the 3-step catalyst is confirmed to slightly outperform the 1-step and the baseline ones, which show an equivalent behaviour.

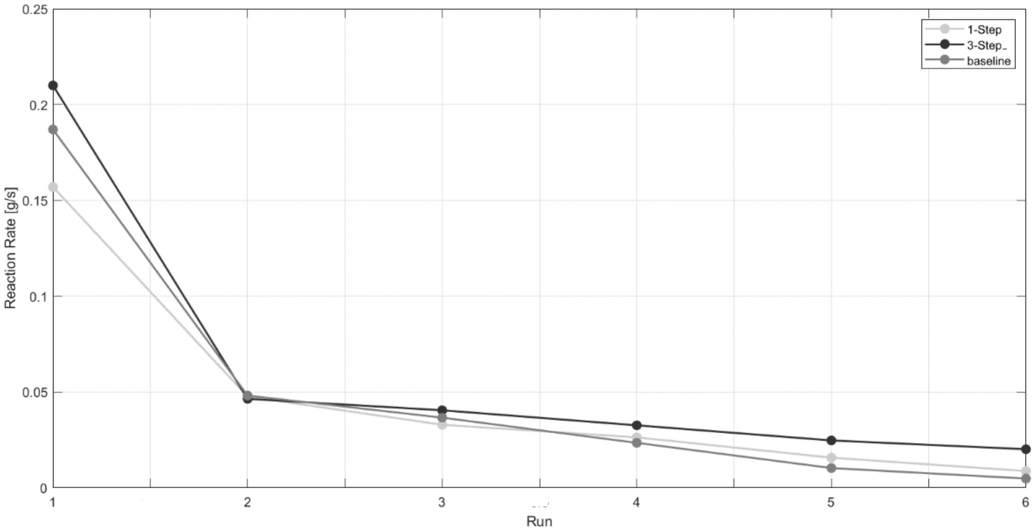

Figure 9: Comparison of produced catalysts reaction rate vs number of runs.

4.2 Decomposer Tests

The baseline catalytic bed has been tested in the decomposition chamber prototype. As shown in Figure 6, temperature and pressure values have been measured at different sections along the decomposer axial direction, employing the reduced configuration - i.e., L/D ≈ 2, with only one catalytic bed module (11) – see Figure 6(b) for details. A nominal mass flow rate of 15 g/s (i.e., bed loading G = 21.22 kg/s/m^2) of HTP stored at 24 bar has been decomposed for a cumulative time of 36 s.

The firing is characterized by an initial transient phase of three short-pulsed runs, lasting between 1 and 2 seconds, aiming at partially pre-heating the catalytic bed. The temperature distributions - see Figure 10(b)- highlight the long transient time required by this kind of catalysts when employed in cold start operations, mostly because of their low surface area. Nevertheless, during the first long run (~ 10 s), the lower part of the catalyst bed appears to have reached a steady state condition in terms of temperature, which is on the contrary achieved inside the post-chamber during the second steady long run. In general, the temperature in the post-chamber T_4 is always lower than T_3, probably because of thermal losses between these two sections introduced by the catalyst bed retainer plate.

Both pressure and temperature at sections 3 and 4 along the prototype present steady profiles, suggesting that the catalyst is efficiently decomposing the liquid HTP without showing sign of deterioration. As shown in Figure 10(a), a small pressure drop across the injection plate is achieved, as nominally designed (i.e., nominal $\Delta P_{inj} \sim 0.5$ bar) in order to obtain low injection velocity. Similarly, small pressure drops across the catalytic bed are measured, showing no occlusion caused by structural damage of the pellets.

The temperature efficiency, as defined in Eq. (3), is used for evaluating the effectiveness of catalytic beds in decomposing HTP:

$$\eta_{\Delta T} = \frac{T_{exp} - T_{amb}}{T_{ad} - T_{amb}} \tag{3}$$

where T_{exp} is the measured value, T_{amb} is the ambient temperature and T_{ad} is the adiabatic decomposition temperature. The latter value for 83.5% hydrogen peroxide is 861°C in the present operating conditions. In the present test, the measured values never reached the theoretical one, leading to a maximum efficiency of 88% in the last four runs (i.e, considering the highest temperature value among T_3 and T_4).

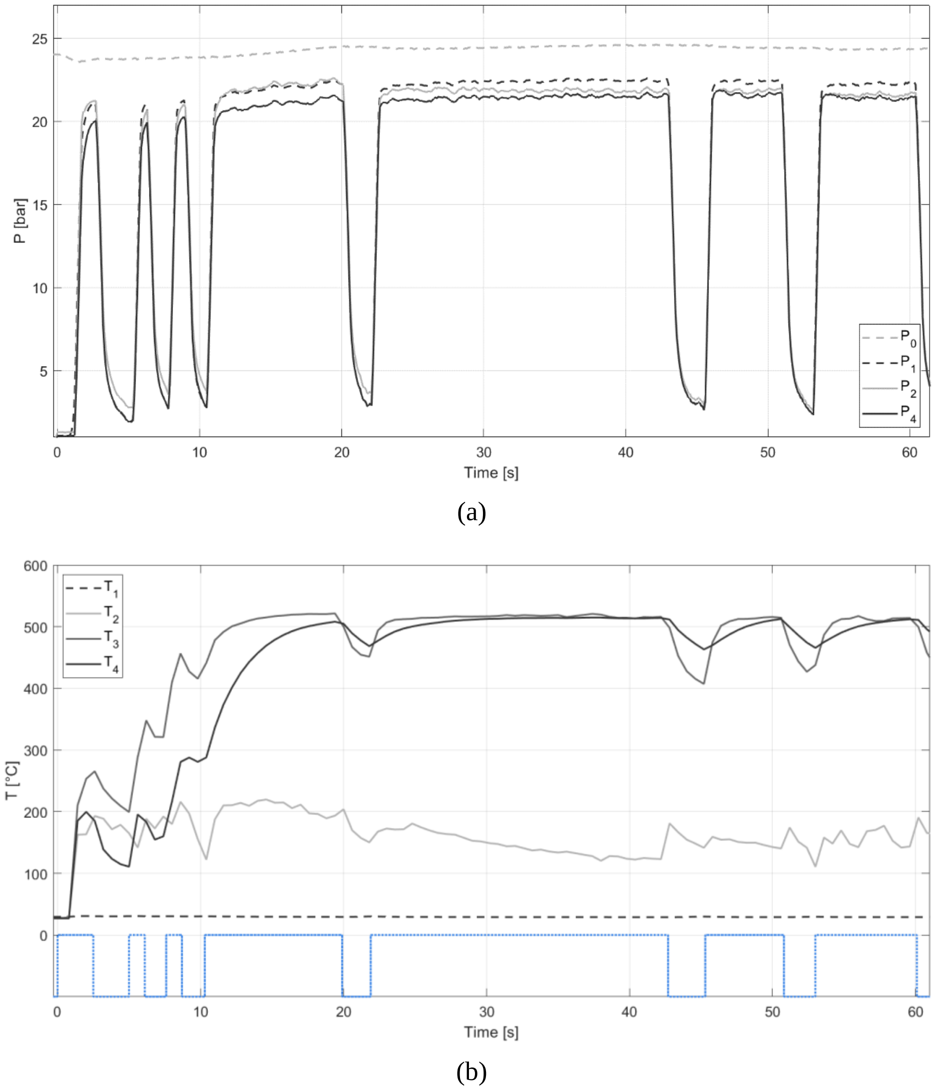

Figure 10: Pressure and temperature distributions during pulsed and continuous tests. The light blue line indicates the opening of the HTP valve.

During the first three cold starts pulses, the maximum temperature is always lower, progressively increasing with each subsequent firing. The upstream catalyst bed T_2 remained approximately around 150-200°C. As in the case of the endurance lab-scale tests, the temperature may be limited to hydrogen peroxide boiling limit at high pressure. However,

the highlighted strong fluctuations probably indicate a concurrent effect between HTP boiling and liquid HTP flooding in the upper part of the bed. Future work shall focus on the characterization and, eventually, on the optimization of the injection head to verify if this effect is related to a non-uniform liquid injection distribution.
The inspections of the catalysts after the tests qualitatively highlighted the effect of the HTP decomposition process. Despite the low injection velocity, the MnOx active phase was partially removed from the catalysts by the liquid propellant in the upstream part of the catalyst bed - see Figure 11 (a) - highlighting the occurrence, even though with limited strength, of the so-called washout process. In general, the mass of the catalyst pack decreased of about 1.45%, highlighting a limited active phase consumption.

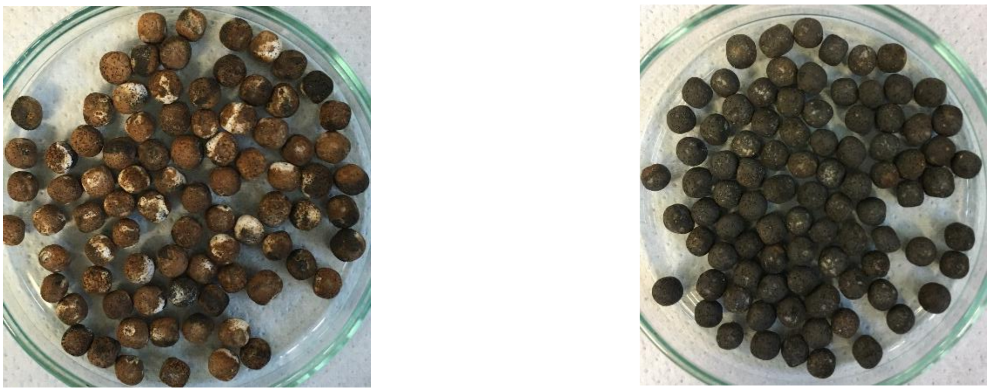
(a) (b)

Figure 11: Post-decomposition catalysts: (a) in the upper part and (b) in the bottom part of the catalyst bed.

5. Conclusion

The paper describes the preparation, characterization, and testing of alumina-supported manganese oxide catalysts. Three different impregnation processes using potassium permanganate as precursor in aqueous solution have been discussed and their results in terms of mass loading and endurance have been presented. In particular, the large mass loading obtained for repeated impregnation and calcination steps enables to increase the endurance of the catalysts when tested at lab-scale level. This aspect is a promising result if considering that in real environment testing the upstream layer of the baseline bed (i.e., no repeated impregnation steps) suffered from partial washout. Thus, further investigations are recommended to verify this promising behaviour.

Pulsed and long burn steady state behaviours have been investigated during a single cold start test in a decomposition chamber prototype operating with 15 g/s of 83.5% HTP. A temperature-efficiency of 88% was achieved during the steady state regime, while lower performances were obtained during the initial pulsed operations, mainly aimed at pre-heating the catalyst bed. The catalyst was able to work properly for a cumulative amount of time equal to 36 s and the packed bed inspection after the test highlights a contained mass decrease, suggesting that additional firings are possible.

Acknowledgment

The authors gratefully acknowledge the contribution of Mr. Valerio Gaioni and *NumeriCAE* to the design of the decomposition chamber and of Mr. Alberto Verga to the implementation of the decomposer assembly. This work was partially supported by Avio S.p.A. within the frame of the LIBRE project, Contract N. I201329. The authors would like to express their gratitude to Andrea Braghieri, Giacomo D'Agostini and Lorenzo Palimento who have participated in various aspects of the study.

References

[1] Bombelli, V., Simon, D., Moerel, J. L. and Marée, T. 2003. Economic Benefits of the use on Non-Toxic Monopropellants for Spacecraft Applications. AIAA Paper N. 2003-4783.
[2] Maggi, F., Carlotti, S. and Gaioni, V. 2021. Preliminary assessments for the development of a green storable bipropellant rocket engine based on H2O2. In: 7th Space Propulsion Conference 2020+1 (SP20+1).
[3] Rarata, G. and, Rokicka, K. 2015. The Manganese Oxides Decomposition Catalysts for Highly Concentrated Hydrogen Peroxide. In: Transactions of the Institute of Aviation, 3, pp. 49–57.

DOI: 10.13009/EUCASS2022-6184

[4] Guseinov Sh. L, Fedorov, S. G., Kosykh, V. and Storozhenko, P. 2020. Hydrogen Peroxide Decomposition Catalysts Used in Rocket Engines. In: Russian Journal of Applied Chemistry 93(4), pp. 467–487.

[5] Sorge, A. R., Turco, M., Pilone, G., and Bagnasco, G. 2004. Decomposition of hydrogen peroxide on MnO2/TiO2 catalysts". Journal of Propulsion and Power, 20(6), pp. 1069-1075.

[6] Pędziwiatr, P. 2018. Decomposition of hydrogen peroxide-kinetics and review of chosen catalysts. Acta Innovations, (26), pp. 45-52.

[7] Su-Lim, L., and Choong-Won, L. 2009. Performance Characteristics of Silver Catalyst Bed for Hydrogen Peroxide. Aerospace Science and Technology, 13(1), pp. 12–17.

[8] Dolci, S., Amico, D. B. D., and Alta, S. A. 2015. Platinum Catalysts Development for 98 % Hydrogen Peroxide Decomposition in Pulsed Monopropellant Thrusters. Journal of Propulsion and Power, 31(4), pp. 1204–1216.

[9] An, S., and Kwon, S. 2009. Scaling and Evaluation of Pt/Al2O3 Catalytic Reactor for Hydrogen Peroxide Monopropellant Thruster. Journal of Propulsion and Power, 25(5), pp. 1041-1045.

[10] Shu-Sung, L., and Mirat, D. G. 1998. Catalytic Decomposition of Hydrogen Peroxide on Iron Oxide: Kinetics, Mechanism, and Implications. Environmental Science and Technology, 32, pp. 1417–1423.

[11] Surmacz, P., Kostecki, M., Gut, Z., and Olszyna, A. 2019. Aluminum Oxide–Supported Manganese Oxide Catalyst for a 98% Hydrogen Peroxide Thruster. Journal of Propulsion and Power, 35(3), pp. 614-623.

[12] Jo, S. 2016. Response Characteristics of H2O2 Monopropellant Thrusters with MnO2 -Mixed PbO Catalyst. Aerospace Science and Technology, 60, pp. 1–8.

[13] Kang, S., Lee, D., and Kwon, S., 2021. Manganese Oxide Lanthanum-Doped Alumina Catalyst for Application in Wt. % Hydrogen Peroxide Thruster. CEAS Space Journal, 13, pp. 189–196.

[14] Quintens, H., Boust, B., Bellenoue, M., Beauchet, R., and Batonneau, Y. 2022. Experimental Comparison of Hydrogen Peroxide Catalysts for a Hydrogen Peroxide⁄n-Decane Bipropellant Combustor. Journal of Propulsion and Power.

[15] Torre, L., Pasini, A., Romeo, L., Cervone, A., and D'Agostino, L. 2009. Performance of a Monopropellant Thruster Prototype Using Advanced Hydrogen Peroxide Catalytic Beds. Journal of Propulsion and Power, 25(6), pp. 1291–1299.

[16] Ryan, C. N., Fonda-Marsland, E., Roberts, G. T., Lear, A., Fletcher, E., Giles, L., Dean, W., and Palmer, M. J. 2020. Experimental Validation of a 1- Newton Hydrogen Peroxide Thruster. Journal of Propulsion and Power, 36(2), pp. 1–9.

[17] Scharlemann, C., Schiebl, M., Kappenstein, C., Batonneau, Y, et al. 2006. Development and test of a miniature hydrogen peroxide monopropellant thruster. AIAA Paper N. 2006-4550.

[18] Palmer, M., J., Roberts, G., T., and Musker, A., J. 2011. Design, Build and Test of a 20N Hydrogen Peroxide Monopropellant Thruster. AIAA Paper N. 2011-5697.

[19] An, S., Jin, J., Lee, J., Jo, S., Park, D., and Kwon, S. 2011. Chugging Instability of H 2 O 2 Monopropellant Thrusters with Reactor Aspect Ratio and Pressures. Journal of Propulsion and Power, 27(2), pp. 422–430.

[20] Palmer, M., J. 2014. Experimental Evaluation of Hydrogen Peroxide Catalysts for Monopropellant Attitude Control Thrusters. PhD Thesis, University of Southampton.